INTERFACE

rsif.royalsocietypublishing.org

Research

Cite this article: Sutherland KR, Weihs D. 2017 Hydrodynamic advantages of swimming by salp chains. *J. R. Soc. Interface* **14**: 20170298.
http://dx.doi.org/10.1098/rsif.2017.0298

Received: 22 April 2017
Accepted: 6 July 2017

Subject Category:
Life Sciences–Physics interface

Subject Areas:
biomechanics, biomimetics

Keywords:
multi-jet, propulsion, locomotion, efficiency, pelagic tunicate

Author for correspondence:
Kelly R. Sutherland
e-mail: ksuth@uoregon.edu

Electronic supplementary material is available online at https://dx.doi.org/10.6084/m9.figshare.c.3827929.

THE ROYAL SOCIETY PUBLISHING

Hydrodynamic advantages of swimming by salp chains

Kelly R. Sutherland[1] and Daniel Weihs[2]

[1]Oregon Institute of Marine Biology, University of Oregon, Eugene, OR, USA
[2]Department of Aerospace Engineering and Autonomous Systems Program, Technion, Haifa, Israel

KRS, 0000-0001-6832-6515

Salps are marine invertebrates comprising multiple jet-propelled swimming units during a colonial life-cycle stage. Using theory, we show that asynchronous swimming with multiple pulsed jets yields substantial hydrodynamic benefit due to the production of steady swimming velocities, which limit drag. Laboratory comparisons of swimming kinematics of aggregate salps (*Salpa fusiformis* and *Weelia cylindrica*) using high-speed video supported that asynchronous swimming by aggregates results in a smoother velocity profile and showed that this smoother velocity profile is the result of uncoordinated, asynchronous swimming by individual zooids. *In situ* flow visualizations of *W. cylindrica* swimming wakes revealed that another consequence of asynchronous swimming is that fluid interactions between jet wakes are minimized. Although the advantages of multi-jet propulsion have been mentioned elsewhere, this is the first time that the theory has been quantified and the role of asynchronous swimming verified using experimental data from the laboratory and the field.

1. Introduction

Salps are barrel-shaped marine invertebrates (Phylum Chordata, Class Thaliacea) that swim using a pulsatile jet (figure 1; electronic supplementary material, Movie S1 and S2). Water is drawn in through an oral siphon and subsequent contraction of circular muscle bands ejects water from the posterior atrial siphon to propel the animal forwards. While jet propulsion is not unique to salps—cnidarian jellyfish [1] and cephalopods [2,3] also swim using pulsed jets—salps are unusual in having a two-part life cycle comprising an asexually reproducing solitary stage and a sexually reproducing aggregate stage (figure 1). Aggregate-stage salps are genetically identical zooids that are connected in a chain and swim together as a unit through the coordination of multiple jets [4,5]. The presence of solitary and aggregate stages provides an ideal system for testing whether there are hydrodynamic advantages to swimming using multiple jets.

Individual salps can increase the thrust produced by periodic expulsion of water by tens of per cent compared to a continuous jet with the same ejected momentum. This increased thrust has been described as arising from the formation of discrete vortex rings, which interact positively, reducing losses [3]. This prediction has since been verified with squid in the laboratory and with salps in the natural environment [5,6]. The influence of periodicity on the efficiency of jet motion has been pointed out in other areas, as for example, in studies of periodically emitting smokestacks [7].

These previous studies focused on the thrust produced, but did not consider important side effects: drag is also increased when a body moves by periodically accelerating and decelerating. The drag increase results from a combination of two effects: (i) the periodic formation and release of a viscous boundary layer along the body, and (ii) the acceleration reaction, which does not occur during steady, time-independent motion. This drag penalty may negate the thrust advantage of pulsatile swimming.

This study offers a possible explanation for organisms with multiple zooids, where each individual can propel itself periodically, but the whole group moves

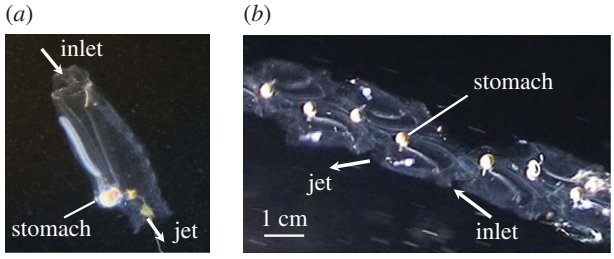

Figure 1. (*a*) *Weelia cylindrica* oozooid and (*b*) blastozooid stage. Note that one zooid is absent in (*b*). For movies of swimming *W. cylindrica*, see electronic supplementary material. (Online version in colour.)

at a constant speed by averaging the thrust at each instant. Thus, the thrust advantages of periodic expulsion of water are preserved, while reducing the losses due to the drag increment mentioned above. However, maintenance of constant speed should require asynchronous swimming by zooids because synchronous swimming (i.e. all zooids pulsing simultaneously) will produce unsteady swimming. Previous studies suggested that normal forward swimming by salp chains (*Salpa fusiformis*) was characterized by uncoordinated, asynchronous swimming [4] that resulted in a lack of pattern in the timing of jet production. It has recently been shown in a laboratory set-up that in-phase pulsing jets have lower thrust when closely spaced and this reduction is significant at the distances observed in salp chains [8]. This finding underscores the advantage of out-of-phase, especially anti-phase, jetting.

Here, we examine the combined effect of thrust and drag, showing that swimming in chains can combine the advantages of periodic thrust, while minimizing the effect of the drag increment due to instantaneous velocity changes. This hydrodynamic advantage is obtained by coordinating the phase difference of ejection of the jets so that, on average, the chain produces an almost uniform, steady velocity. Experimental data of salps swimming in the laboratory and in the natural environment support these assumptions and provide additional insight into how multiple jets are coordinated. Though different salp species exhibit a diversity of chain architectures, including wheel-shaped, transverse and linear chains, this study focuses on two species with linear geometries—*S. fusiformis* and *Weelia cylindrica*. Linear forms are known to produce the highest swimming speeds [9].

The goals of the present study were to (i) examine the theory explaining the combined effect of thrust and drag in individual versus aggregate salps, (ii) verify with experimental data that aggregate salps swim at a relatively constant speed when compared to solitary counterparts, (iii) analyse the volume flow rates produced by pulsing aggregates to examine how swimming is coordinated, and (iv) to observe the timing and formation of pulsed jets produced by aggregate chains *in situ*. Understanding the coordination of multiple jets improves our understanding of principles governing effective locomotion and can potentially inform the design of underwater vehicles.

2. Results

2.1. Theoretical analysis of hydrodynamic advantages

Salps swim at relatively low Reynolds numbers,

$$Re = \frac{UL}{\nu}. \tag{2.1}$$

where U is velocity, L is the length of an individual zooid and ν is the kinematic viscosity. For an aggregate chain of *W. cylindrica*, $Re \sim 5000$ based on mean *in situ* swim speeds of 9 cm s^{-1}, individual zooids approximately 1 cm in length and seawater viscosity ($\nu = 1.83 \times 10^{-6}$ m^2 s^{-1} at 20°C) [9]. Therefore, a relatively thick boundary layer is formed and re-formed during each cycle of jet emission and resting. Pulse frequencies are up to 3 Hz, so a fully developed steady state is probably never fully achieved. At the Reynolds numbers experienced by salps, the drag due to body speed periodically varying with time (D_v) is larger than the drag of the same body moving at constant speed (D_c) as transient acceleration effects [10] are still present.

First considering the steady component only, at these Reynolds numbers a laminar boundary layer is produced on the outer surface of the salp, which can be roughly modelled as a cylinder. For a cylinder, the total drag force over a period T is

$$D_C = 0.5\rho A T U^2 C_D = KATU^2, \tag{2.2}$$

where ρ is the seawater density, A is the wetted area of the animal and C_D is the steady drag coefficient. The drag coefficient does not vary with speed for the reported range of salp swimming speeds [5,9], for both two- and three-dimensional bodies [11]. The exponential decrease in speed during the coast portion of the cycle indicates that one can use a constant drag coefficient during coasting [12] and, for the burst segment, the speed of solitary zooids grows at a decreasing rate that can be attributed to the constant drag coefficient.

Now, looking at periodic speed changes in a single salp, the drag increases due to two effects: the drag, which is proportional to the instantaneous speed, and the added mass (or, as sometimes called, the acceleration reaction).

The velocity change during a single jetting cycle can be expressed as a fraction of the average speed ($V = U_{max} - U_{min}/2U_{av}$, where U_{max} is the maximum velocity, U_{min} is the minimum velocity and U_{av} is the average velocity), and the instantaneous drag can be simplified as being proportional to the speed squared (i.e. assuming that the instantaneous drag dependence on speed is equal to the drag under steady conditions at the same speed). The total drag over a period T is [12]

$$\begin{aligned} D_V &= KA\int_0^T [U(t)]^2 \mathrm{d}t + \frac{m(1+\mu)}{T}\int\left(\frac{\mathrm{d}U}{\mathrm{d}t}\right)\mathrm{d}t \\ &= D_{V1} + D_{V2}, \end{aligned} \tag{2.3}$$

where A is taken to be independent of speed (this assumption will be examined below), m is the animal mass, μ is the added mass coefficient and T is now the cycle period. The function $U(t)$ can be anything between a harmonic (sinusoidal) function and a step function ($U = U_{max}$ for $0 < t < T/2$ and $U = U_{min}$ for $T/2 < t < T$) and is a constant for steady swimming. The limits of integration are not specified in equation (2.3) as integration over full cycles of a periodic function may lead to unrealistic cancellations. Note that the total drag over the period D_{Vi} has units of force × time. Calculating the contribution of D_{V1}

$$D_{V1} = KA\frac{T}{2}(U_{max}^2 + U_{min}^2), \tag{2.4}$$

while

$$D_C = KATU_{av}^2. \tag{2.5}$$

For the step function

$$\left.\begin{aligned} U_{\max} &= U_{\mathrm{av}}\left(1+\frac{V}{2}\right) \\ \text{and}\quad U_{\min} &= U_{\mathrm{av}}\left(1-\frac{V}{2}\right). \end{aligned}\right\} \tag{2.6}$$

So

$$\begin{aligned} D_{V1} &= KAT\frac{U_{\mathrm{av}}^2}{2}\left[\left(1+\frac{V}{2}\right)^2+\left(1-\frac{V}{2}\right)^2\right] \\ &= KATU_{\mathrm{av}}^2(1+V^2) \end{aligned} \tag{2.7}$$

and

$$\frac{D_{V1}}{D_{\mathrm{C}}} = (1+V^2). \tag{2.8}$$

As a simple numerical example, take a case where the salp moves at a maximum velocity of 9 cm s^{-1} for one half-period and 3 cm s^{-1} for the other half, for a peak to peak difference of 6 cm s^{-1} and an average speed of 6 cm s^{-1}, so $V = 0.5$ and the drag increment is 25%.

We now apply another speed profile, a sinusoidal cyclical motion, where

$$U(t) = U_{\mathrm{av}}\left(1+\frac{V}{2}\sin\omega t\right). \tag{2.9}$$

In this case, it can be shown that the ratio

$$\frac{D_{V1}}{D_{\mathrm{c}}} = \left(1+\frac{\pi V^2}{8}\right). \tag{2.10}$$

In our example with $V = 0.5$ the gain is only 10%.

Next, we look at the relative contribution of the added mass (acceleration reaction), D_{V2}.

From (2.3)

$$D_{V2} = m(1+\mu)\left(\frac{\mathrm{d}U}{\mathrm{d}t}\right) = \rho W(1+\mu)\left(\frac{\mathrm{d}U}{\mathrm{d}t}\right), \tag{2.11}$$

which, unfortunately, through m and especially μ, is highly specific to animal shape and water through-flow speed. So we take the volume W to be 3×10^{-4} m^3 and a cycle time of 0.3 s (table 1 and figure 5), $V = 0.5$, $\mu = 0.2$ [13], with the slenderness ratios (1.5–3) taken from Madin [9] and the acceleration as the speed difference (0.06 m) divided by half a cycle time (0.17 s) to arrive at a rough value of 1.3×10^{-5} kg m s^{-2}. The constant speed drag, using the same rough data, and a drag coefficient based on a frontal area of 0.5 results in a value of about 18×10^{-5} kg m s^{-2}, i.e. the ratio $D_{V2}/D_{c'}$ which for the sinusoidal speed variation is

$$\rho A^{1.5}(1+\mu)\frac{V}{2}\omega\cos\omega t. \tag{2.12}$$

So that

$$\frac{D_{V2}}{D_{\mathrm{c}}} = \frac{1.3}{18} = 0.072. \tag{2.13}$$

Moreover, the acceleration drag contribution is less but not negligible. This estimate needs to be qualified, as during periods of flow through the animal, the added mass coefficient μ is much smaller.

Bone & Trueman [4] provide a comprehensive set of data from which another estimate of the drag increment may be made. The acceleration phase is at higher drag—Bone & Trueman [4] estimate the ratio to be up to 1.9 for solitaries, but to be much less (<1.3) for aggregates. This provides another advantage of swimming at roughly constant speeds, as at low swimming speeds, and low maximum to minimum drag ratios, the energetic cost of periodic speed changes can be higher than swimming at constant speed ([12], figure 2, for example).

The assumption made above that the wetted area is constant during the whole cycle needs to be discussed, as the salp takes in a large amount of water (20–30% of body volume) to produce the jet. As the external area of a cylinder is linearly proportional to the radius, and the volume enclosed varies as the square of the radius, this corresponds to a roughly 10–20% increase in surface area for the fully 'filled' salp. However, when actively swimming, the fluid is taken in during the lowest part of the velocity cycle, and quickly ejected to produce the jet, so that for most of the period, the smaller volume is found, and the assumption is thus justified.

An additional contribution to drag reduction in a chain is the fact that parts of the circumference do not come in contact with the water. While the conjoined area has never been measured accurately, in a transverse chain, a conservative estimate based on stills and videos of such chains is that the hidden area is at least 10% per lateral partner, or 20% for each member except for those at the ends. The wetted area that the chain presents to the flow is thus reduced, and from equation (2.1) a 20% decrease in total drag is obtained for large linear chains. For linear chains, this proportion may be higher still, especially as the jets ejected by individuals are tilted diagonally outwards, so that the body of the following individual is less exposed to the oncoming flow.

Another, probably less significant contribution to drag reduction is the fact that volume changes by 11–27% during jetting [15], causing periodic radial flows of 3–8% that add up. This can also be estimated from the body length change by assuming a constant volume. Data from Bone & Trueman [4] show a body height change of approximately 6%, which translates to an approximately 3% diameter change from this effect. This contribution will mainly affect linear chains and will probably be a much smaller contribution to drag reduction than the other sources.

2.2. Swimming kinematics of *Salpa fusiformis* and *Weelia cylindrica*

Experimental observations in the laboratory of swimming *S. fusiformis* from Bone & Trueman [4] show that pulsatile swimming by single salps produces unsteady swimming where velocity increases during jet production and decreases during the refill period (figure 2). This unsteady pattern replicates a burst and coast mode of swimming as seen in fish [12,14] zooplankton [16] and crustaceans [17], and is observed in both solitary-stage salps and individual aggregate-stage salps that have broken off from a chain. Swimming by an eight-member aggregate chain when all individuals were pulsing resulted in a much smoother velocity profile than the velocity profile exhibited by the same chain when a single individual was actively pulsing

Table 1. Parameters and fit of sine curves representing volume change during swimming in eight zooids shown in figure 5. The mean of each parameter (MEANS) and curve fit parameters produced from a mean of all zooids (aggs. 1–8 black line in figure 5*b*) are also shown.

	sine curve parameters					ANOVA		
aggregate	*a* (ml)	*b* (s)	*c* (s)	y_0 (ml)	R^2	*F*	*p*	d.f.
1	0.01	0.33	1.63	0.31	0.67	41.42	<0.0001	65
2	0.02	0.35	5.23	0.30	0.83	99.77	<0.0001	65
3	0.01	0.37	0.24	0.31	0.65	37.90	<0.0001	65
4	0.01	0.34	2.91	0.30	0.78	74.13	<0.0001	65
5	0.01	0.30	3.45	0.29	0.73	55.72	<0.0001	65
6	0.01	0.33	4.65	0.30	0.73	55.77	<0.0001	65
7	0.01	0.30	5.20	0.31	0.35	11.21	<0.0001	65
8	0.01	0.31	1.39	0.30	0.81	86.05	<0.0001	65
MEANS	*0.013*	*0.33*	*3.09*	*0.30*				
aggs. 1–8	0.005	0.35	4.60	0.30	0.87	584.50	<0.0001	256

(figure 3). Active pulsing by all members also produced an overall higher swimming velocity of the chain (figure 3).

Laboratory swimming kinematics of eight *W. cylindrica* zooids from a chain during 'normal' forward swimming revealed an asynchronous pulsing pattern. The time-varying volume change curves were well approximated by a four-parameter sine curve (figure 4). For all eight curves the four fitting parameters approximated the raw data successfully (R^2 values and ANOVA statistics are given in table 1). The baseline parameter, y_0, represents the average volume of a zooid (ml) and *b* is the pulse time (s per pulse). The amplitude *a* represents the volume change from the baseline but was probably an underestimate because, in some cases, the peak volumes were not captured by the sine fit (figure 4).

The curves showed asynchronous swimming and, as a result of the different individual pulse patterns by the eight zooids, the volume flow rate of the chain as a whole was relatively smooth over time (figure 5). Investigating a subset of the zooids (1–4 in figure 5*c* and 5–8 in figure 5*d*) reveals that the specifics of the pulse patterns and how they interact can result in a relatively variable (figure 5*c*) or relatively smooth volume flow rate (figure 5*d*). Examination of the pulse rates of individual zooids (table 1, pulse rate $= 1/b$) shows that each zooid had a unique pulse rate that was offset from its neighbours; these slight offsets explain the asynchrony in swimming. The lack of apparent pattern or coordination of pulse rates still achieves a relatively smooth velocity profile.

To find an independent estimate of the drag coefficient, we use eq. 24b from Weihs [12], which shows that the time spent during the coast phase varies with the decrease in speed during the coast phase. We chose this because the coast phase of burst and coast swimming is longer, so the measurement error in time, from figure 2, is smaller.

The distance is ([12], eq. 24b)

$$t_{co} = \frac{m}{c}\left(\frac{1}{U_i} - \frac{1}{U_f}\right) = \frac{2\rho V}{\rho A_w C_{DW}}\left(\frac{1}{U_i} - \frac{1}{U_f}\right). \tag{2.14}$$

So

$$C_{DW} = \frac{2V}{A_w t_{co}}\left(\frac{1}{U_i} - \frac{1}{U_f}\right), \tag{2.15}$$

where t_{co} is the time spent during coasting, *m* and *V* are the salp mass and volume, respectively, A_W is the wetted area, C_{DW} is the drag coefficient based on the wetted area, and U_f and U_i are the speeds at the beginning and the end of the coast section of the cycle.

We can examine an example case of coasting from figure 2*b*, between $t = 0.16$ and 0.5 s, where the speed decreased from 8.5 cm s^{-1} to 1.7 cm s^{-1}. To simplify the calculation, we estimate the oozooid to be, on average, a sphere of 3 cm radius, using the expressions for spherical volume and surface area.

We arrive at a drag coefficient of 0.025 based on the wetted area, which is of the right order of magnitude. Obviously, more accurate measurements need to be made, but this is beyond the scope of this paper.

2.3. *In situ* wake visualizations of *Weelia cylindrica*

In situ flow visualizations with fluorescein dye revealed the formation of multiple jets produced by *W. cylindrica* during asynchronous swimming (figure 6; electronic supplementary material, Movie S3). Individual jets were produced from discrete locations at each atrial siphon and at discrete points in time due to offsets in pulse frequencies (figure 5), resulting in non-interacting jet wakes.

3. Discussion

Taken together, theory and experimental data support that salp chains with multiple swimming units have a substantial hydrodynamic advantage over solitary forms. Previous studies have hinted at the hydrodynamic benefits of swimming with multiple units in salps [4,5,9,15] and siphonophores [18,19], but a robust quantitative analysis was lacking until now. Here, we have shown the hydrodynamic advantage of swimming with multiple jets in terms of drag reduction, and also begin to demonstrate the coordination of those jets (figure 5) and the consequences in terms of wake interactions (figure 6).

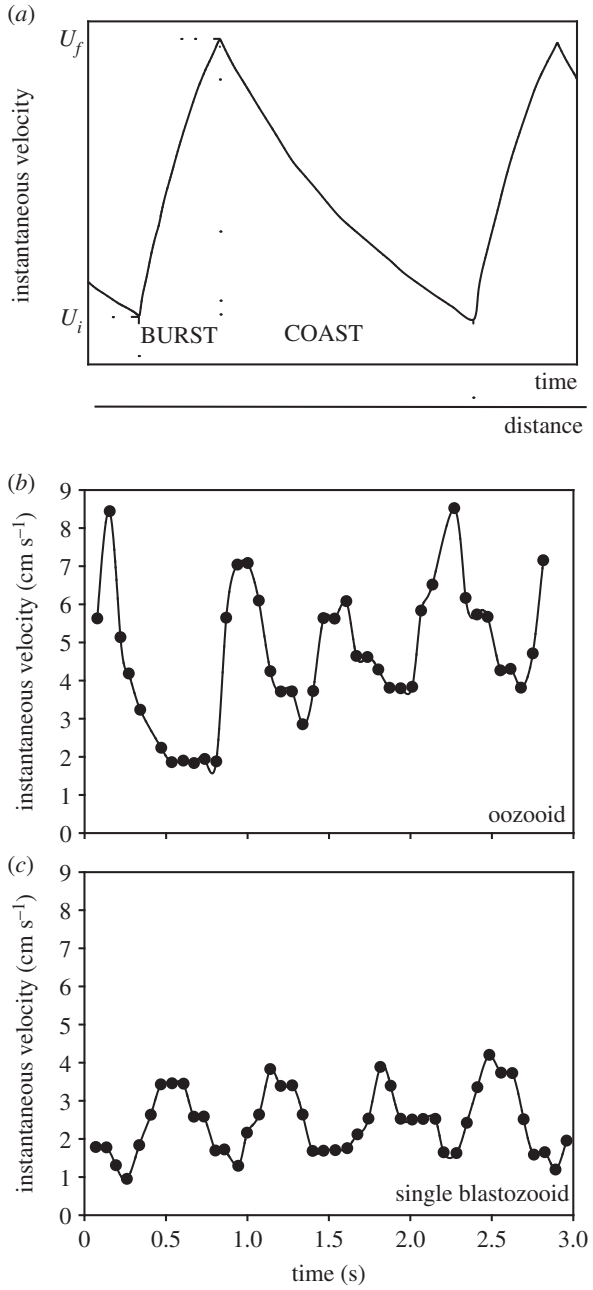

Figure 2. Pulsatile jetting by a single individual produces a burst and coast velocity profile; (*a*) a conceptual diagram (modified from [14]), (*b*) *Salpa fusiformis* oozooid and (*c*) a single *S. fusiformis* blastozooid (*b* and *c* modified from [4]).

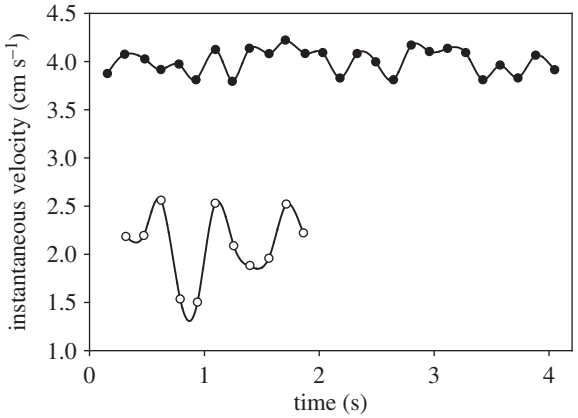

Figure 3. Steady swimming in an eight-member *S. fusiformis* aggregate, with all individuals actively pulsing (solid circles) and unsteady swimming produced by a single individual pulsing (open circles) (modified from [4]).

Stereotypical burst and coast swimming (figure 2) is common in aquatic invertebrates and swimming with multiple propulsors can potentially produce a smoother velocity profile. However, if all zooids pulse synchronously, the less efficient burst and coast pattern is conserved. Asynchronous swimming is therefore required to derive these hydrodynamic benefits. Asynchronous swimming may be coordinated—examples include the metachronal waves generated by pleopods in swimming krill [20] and comb rows in ctenophores [21]—or, it may be uncoordinated as was previously suggested for salps [4]. Our results confirm that 'normal', forward swimming is uncoordinated in salps and the pattern arises from individual differences in pulse frequencies and phase shifts (table 1, figure 5). There are advantages of uncoordinated, asynchronous swimming. First, though salp chains have neurological connections between zooids, uncoordinated swimming does not require neurological integration between swimming units. Second, the chain is robust to the loss of individuals within the chain (figure 1*b*) or to shortening of the chain. At some minimum number of zooids, uncoordinated swimming will no longer reliably produce steady swimming. For example, 'beating' effects where individual pulses become synchronized momentarily can produce spikes in thrust production (figure 4*c*). A more detailed understanding of the minimum number of zooids and the combination of parameters that optimizes steady swimming presents an interesting area of future investigation.

Earlier work on the neurophysiology of salps is consistent with our observations of their swimming coordination. Each individual salp has a dorsal brain composed of motor neurons and 'pacemaker' neurons [22]. The firing rate of pacemaker neurons is directly influenced by action potentials generated from the epithelial sensory system (skin impulses) and from a simple eye [23], which in turn probably determines the firing rate of the motor neurons [24]. Interestingly, the firing rate of the pacemaker neurons (1–1.7 Hz in *S. fusiformis*, [23]) does not match the locomotory pulse frequency and the details of how pacemaker neurons control the swimming frequency are not completely understood [24]. Nevertheless, the presence of a pacemaker neuron helps explain how the pulse frequency of each individual salp is governed during uncoordinated swimming.

Coordination among blastozooids in a chain is achieved through the transmission of electrical impulses between individuals via attachment plaques [25]. Each blastozooid in a chain has eight attachment plaques. Flow of signals is unidirectional, necessitating two distinct plaque types linking the blastozooid to each neighbour for sending and receiving electrical events [26]. These neurological connections allow for the coordination of synchronous forward and reverse swimming, but synchronous swimming is only observed during escape responses [4]. In response to extreme mechanical stimulation, the chain can break apart so that individuals can swim away individually and are still functional, though this is rare in nature [27].

Asynchronous swimming influences not only the net volume being expelled from the chain but also the degree of wake interactions. *In situ* flow visualizations, especially of linear chains where the jets are tilted outwards (figure 6), demonstrate that jets may not interact substantially

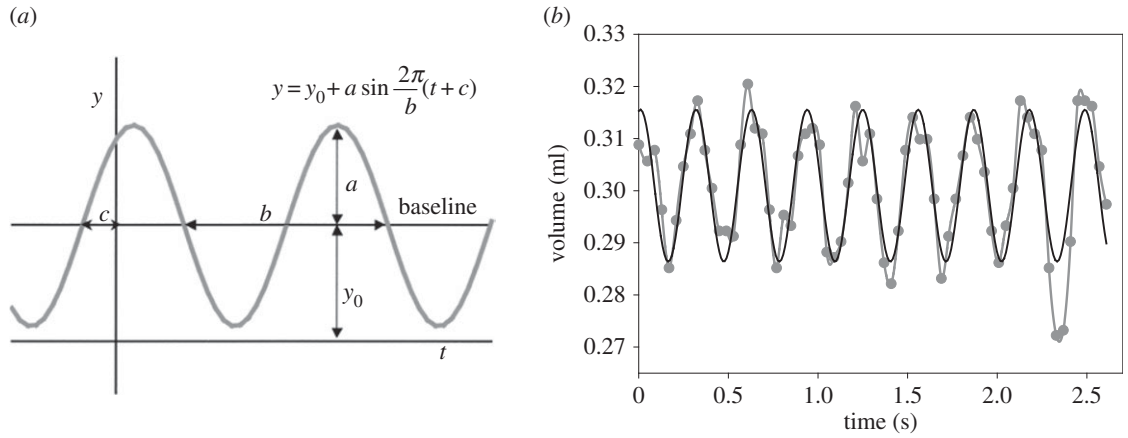

Figure 4. (*a*) Four-parameter sine curve used to approximate volume change during swimming by *W. cylindrica* blastozooids. *a* is the amplitude or change in volume, *b* is the period or pulse time, *c* is the offset and y_0 is the baseline height or mean volume. (*b*) Raw data and sine curve fit for one blastozooid (8).

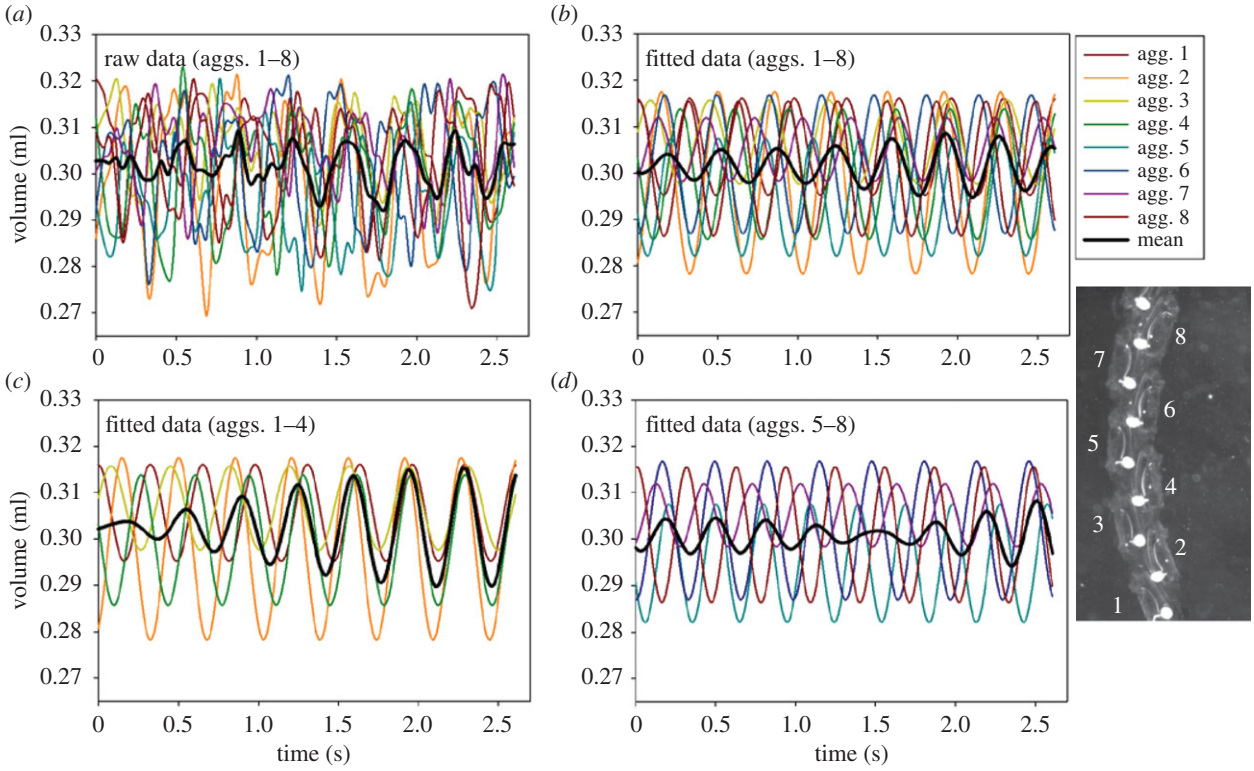

Figure 5. Volume change of eight individual blastozooids during steady swimming by a 16-member *W. cylindrica* aggregate chain with all individuals actively pulsing. (*a*) Raw data and (*b–d*) four-parameter sine curves fitted to raw data (see table 1 for fitting parameters). (*a*) and (*b*) show data for all eight individuals; (*b*) and (*c*) show fitted data for individuals 1–4 and 5–8, respectively. Dark lines show means for individuals in each plot.

during swimming. The production of discrete, non-interacting wakes may provide an added hydrodynamic benefit: laboratory research shows that interactions between closely spaced pulsed jets come at a hydrodynamic cost in terms of decreased thrust [8]. Future research on freely swimming salps could directly investigate whether and to what extent jets interact. Although we have focused on the more linear, streamlined forms here, salp species display a range of chain architectures [9]. The relative position of individuals within the chain as well as the timing of jets will influence hydrodynamic efficiency among the different chain arrangements.

Broadly speaking, coloniality presents a number of potential adaptive advantages. Modular organisms replicate functional roles and can therefore contain damage or the loss of some units (e.g. figure 1*b*). Furthermore, the colony as a whole can depart from allometric constraints faced by a single zooid. A large range of possible colony architectures can arise from a single zooid morphology [28]. Though colonies or organisms with multiple units are relatively common on the sea floor, coloniality is rare in the pelagic realm in spite of the potential hydrodynamic advantages; salps and siphonophores present perhaps the most striking examples [29] and are the only pelagic organisms to our knowledge that use multiple pulsed jets (pyrosomes use continuous jets). Newly released salp chains comprise tens to hundreds of blastozooids [30,31] and depending on individual zooid lengths, which vary among species (3–190 mm; [32]), chains can reach up to 10 metres and still swim effectively in open water (K.R.S. 2009 and 2012, personal observation).

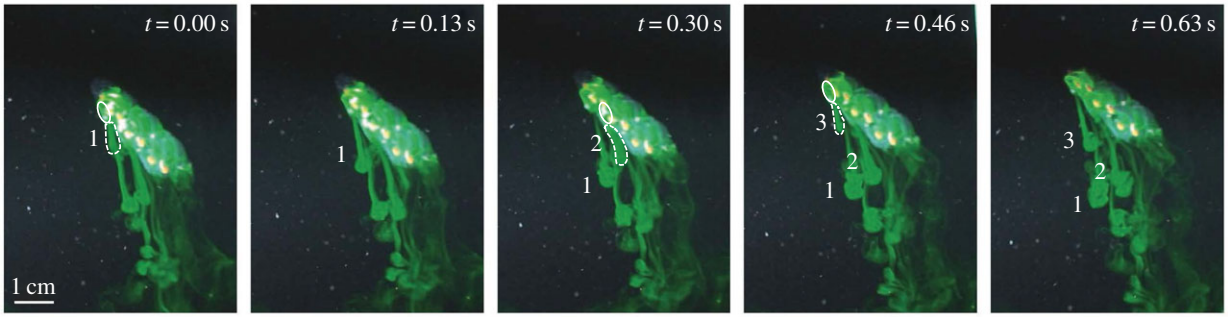

Figure 6. Three developing jets produced by a *W. cylindrica* aggregate chain visualized *in situ* using fluorescein dye. Blastozooid producing jets and jets are circled (solid and dashed lines, respectively) in the first frame that they appear. Jets 1 and 3 emerge from the same zooid and jet 2 emerges from an adjacent zooid. Only developing jets are numbered, but jets produced before $t = 0$ s can also be seen. For full video sequence, see electronic supplementary material, Movie S3.

The locomotory benefits arising from multi-jet propulsion can be considered in the context of ecological roles. The salp species investigated in this study—*S. fusiformis* and *W. cylindrica*—have linear, streamlined forms. Salp species are known to make diel vertical migrations (DVMs) [33] and in the genus *Salpa*, daytime depths can exceed 800 m [34,35], representing some of the largest vertical excursions among marine plankton. A recent global analysis of DVMs showed that typical daytime depths range from 200 to 650 m [36]. The remarkable migratory depths achieved by salps are at least partially explained by their effective locomotion.

Studying the locomotory kinematics that govern swimming efficiency of salp chains sheds light on their behaviour, neurophysiology and ecological roles and can also provide design rules for underwater vehicles. Non-uniform pulse rates among zooids suggest that each zooid is controlled by an individual pacemaker and does not derive a swimming frequency from its neighbours during normal steady-state swimming. This emergent behaviour—steady, hydrodynamically efficient swimming—can inform control variables for salp-inspired multi-jet vehicles. Pulse generators programmed with slight frequency offsets would be sufficient to create relatively steady, asynchronous locomotion and there may be additional benefits in terms of reducing wake interactions.

4. Methods

4.1. Swimming kinematics of *Salpa fusiformis* and *Weelia cylindrica*

Velocity profiles from swimming *S. fusiformis* solitaries and aggregates were extracted from Bone & Trueman [4] to examine whether actively pulsing aggregate chains produced more uniform velocities than solitary-stage salps.

Laboratory and *in situ* swimming observations of *W. cylindrica* were made at the Liquid Jungle Laboratory off the pacific coast of Panama (7°50′ N, 81°35′ W) during January 2009 and April 2012. Specimen collection and *in situ* videography were performed using bluewater diving techniques [5,37]. Thrust production is directly related to the volume expelled during jet formation, and hence in order to examine time-varying thrust, we collected high-speed videos (Photron Fastcam, 125 fps, 1024 × 1024 pixels) of swimming *W. cylindrica* in custom-built glass tanks. Images from sequences where salps were pulsing normally through the centre of the tank were subsequently analysed using Image J (http://rsbweb.nih.gov/ij). Instantaneous volume (V) during swimming by eight individual zooids in a chain was measured over multiple pulse cycles (7–8). Volume measurements were based on a prolate triaxial ellipsoid shape with three semi-axes (r_1, r_2, r_3).

$$V = \frac{4}{3}\pi r_1 r_2 r_3. \tag{4.1}$$

Semi-axes r_1 and r_2 represent the atrial height and width, respectively, and were assumed to be equal during the resting phase between pulses. Semi-axis r_3 represents the zooid length. Atrial height, r_1, decreased during a pulse and increased during relaxation; atrial width and zooid length were assumed not to vary during swimming. Time-varying volume measurements were fitted with a four-parameter sine equation in Sigma Plot 12.5 (Systat Software, Inc.).

$$y = y_0 + a \sin\frac{2\pi}{b}(t + c), \tag{4.2}$$

where y_0 is the height of the baseline or mean volume (ml), a is the amplitude or change in volume, b is the period or pulse time, and c is the offset (s). The fit of each sine curve was assessed with an ANOVA after testing for normality (Shapiro–Wilk) and constant variance. All volume flow data fit the constant variance assumption and though two of the curves did not pass the normality test, a four-parameter sine curve was deemed the best overall fit to the raw data and the parameters provided useful kinematic data.

4.2. Wake visualizations of *Weelia cylindrica*

In situ dye visualizations of swimming *W. cylindrica* were taken with a Sony HDR-HC7 camcorder in an Amphibico housing during night bluewater SCUBA dives [5]. Fluorescein dye was injected into the oral siphons with a micropipette and a 10 W high-intensity discharge light (Light and Motion) was used to illuminate jet wakes.

Data accessibility. Raw data from figure 5*a* have been uploaded to the Biological and Chemical Oceanography Data Management Office (BCO-DMO) and are available at the following link: http://www.bco-dmo.org/project/653245.

Authors' contributions. D.W. and K.R.S. conceived of the study and wrote the manuscript. D.W. developed the theory and K.R.S. conducted the experiments and the analysis.

Competing interests. We declare we have no competing interests.

Funding. We are grateful for funding from the National Science Foundation (OCE-1537201 to K.R.S.), the Sloan Foundation (K.R.S.) and the LFN Fund (D.W.).

Acknowledgements. We are grateful for the comments of two anonymous reviewers that improved the manuscript. We thank Thanasi Athanassiadis and Jack Costello for useful discussions.

References

1. Dabiri JO, Colin SP, Costello JH, Gharib M. 2005 Flow patterns generated by oblate medusan jellyfish: field measurements and laboratory analyses. *J. Exp. Biol.* **208**, 1257–1265. (doi:10.1242/jeb.01519)
2. Anderson EJ, Grosenbaugh MA. 2005 Jet flow in steadily swimming adult squid. *J. Exp. Biol.* **208**, 1125–1146. (doi:10.1242/jeb.01507)
3. Weihs D. 1977 Periodic jet propulsion of aquatic creatures. *Fortschr. Zool.* **24**, 171–175.
4. Bone Q, Trueman ER. 1983 Jet propulsion in salps (Tunicata: Thaliacea). *J. Zool. Lond.* **20**, 481–506. (doi:10.1111/j.1469-7998.1983.tb05071.x)
5. Sutherland KR, Madin LP. 2010 Comparative jet wake structure and swimming performance of salps. *J. Exp. Biol.* **213**, 2967–2975. (doi:10.1242/jeb.041962)
6. Krueger PS, Moslemi AA, Nichols JT, Bartol IK, Stewart WJ. 2008 Vortex rings in bio-inspired and biological jet propulsion. *Adv. Sci. Technol.* **58**, 237–246. (doi:10.4028/www.scientific.net/AST.58.237)
7. Baker PJ, Jacobs BE. 1971 Pulsed Emission Chimney. *Civil. Eng. Public. Works. Rev.* **66**, 199–201.
8. Athanassiadis AG, Hart DP. 2016 Effects of multijet coupling on propulsive performance in underwater pulsed jets. *Phys. Rev. Fluids* **1**, 034501. (doi:10.1103/PhysRevFluids.1.034501)
9. Madin LP. 1990 Aspects of jet propulsion in salps. *Can. J. Zool.* **68**, 765–777. (doi:10.1139/z90-111)
10. Daniel TL. 1984 Unsteady aspects of aquatic locomotion. *Am. Zool.* **24**, 121–134. (doi:10.1093/icb/24.1.121)
11. Schlichting H, Gersten K. 2000 *Boundary layer theory*, 8th edn. Berlin, Germany: Springer.
12. Weihs D. 1974 Energetic advantages of burst swimming of fish. *J. Theor. Biol.* **48**, 215–229. (doi:10.1016/0022-5193(74)90192-1)
13. Lamb SH. 1932 *Hydrodynamics*, 6th edn. Cambridge, UK: Cambridge University Press and Dover, NY.
14. Videler JJ, Weihs D. 1982 Energetic advantages of burst-and-coast swimming of fish at high speeds. *J. Exp. Biol.* **97**, 169–178.
15. Sutherland KR, Madin LP. 2010 A comparison of filtration rates among pelagic tunicates using kinematic measurements. *Mar. Biol.* **157**, 755–764. (doi:10.1007/s00227-009-1359-y)
16. Haury L, Weihs D. 1976 Energetically efficient swimming behavior of negatively buoyant zooplankton. *Limnol. Oceanogr.* **21**, 797–803. (doi:10.4319/lo.1976.21.6.0797)
17. Spanier E, Weihs D, Almog-Shtayer G. 1991 Swimming of the Mediterranean slipper lobster. *J. Exp. Mar. Biol. Ecol.* **145**, 15–31. (doi:10.1016/0022-0981(91)90003-F)
18. Mackie GO. 1964 Analysis of locomotion in a siphonophore colony. *Proc. R. Soc. Lond. B* **159**, 366–391. (doi:10.1098/rspb.1964.0008)
19. Costello JH, Colin SP, Gemmell BJ, Dabiri JO, Sutherland KR. 2015 Multi-jet propulsion organized by clonal development in a colonial siphonophore. *Nat. Commun.* **6**, 1–6. (doi:10.1038/ncomms9158)
20. Murphy DW, Webster DR, Kawaguchi S, King R, Yen J. 2011 Metachronal swimming in Antarctic krill: gait kinematics and system design. *Mar. Biol.* **158**, 2541–2554. (doi:10.1007/s00227-011-1755-y)
21. Sleigh. 1968 Metachronal co-ordination of the comb plates of the ctenophore Pleurobrachia. *J. Exp. Biol.* **48**, 111–125.
22. Fedele M. 1933 Sul ritmo muscolare somatico delle Salpe. *Boll. Soc. Nat. di Napoli* **45**, 475–478.
23. Mackie GO, Bone Q. 1977 Locomotion and propagated skin impulses in salps (Tunicata: Thaliacea). *Biol. Bull.* **153**, 180–197. (doi:10.2307/1540700)
24. Bone Q, Mackie GO. 1982 Urochordata. In *Electrical conduction and behaviour in 'simple' invertebrates* (ed. GAB Shelton), pp. 473–535. Oxford, UK: Oxford University Press.
25. Bone Q, Anderson PA, Pulsford AN. 1980 The communication between individuals in salp chains I. Morphology of the system. *Proc. R. Soc. Lond. B* **210**, 549–558. (doi:10.1098/rspb.1980.0152)
26. Anderson PA, Bone Q. 1980 Communication between individuals in salp chains II. Physiology. *Proc. R. Soc. Lond. B* **210**, 559–574. (doi:10.1098/rspb.1980.0153)
27. Madin LP. 1974 Field observations on the feeding behavior of salps (Tunicata: Thaliacea). *Mar. Biol.* **25**, 143–147. (doi:10.1007/BF00389262)
28. Hughes RN. 2005 Lessons in modularity: the evolutionary ecology of colonial invertebrates. *Sci. Mar.* **69**, 169–179. (doi:10.3989/scimar.2005.69s1169)
29. Mackie GO. 1986 From aggregates to integrates: physiological aspects of modularity in colonial animals. *Phil. Trans. R. Soc. Lond. B* **313**, 175–196. (doi:10.1098/rstb.1986.0032)
30. Daponte MC, Capitanio FL, Esnal GB. 2001 A mechanism for swarming in the tunicate Salpa thompsoni (Foxton, 1961). *Antarct. Sci.* **13**, 240–245. (doi:10.1017/S0954102001000359)
31. Heron AC, Benham EE. 1985 Life history parameters as indicators of growth rate in three salp populations. *J. Plankton Res.* **7**, 365–379. (doi:10.1093/plankt/7.3.365)
32. Henschke N, Everett JD, Richardson AJ, Suthers IM. 2016 Rethinking the role of salps in the ocean. *Trends Ecol. Evol.* **31**, 720–733. (doi:10.1016/j.tree.2016.06.007)
33. Madin LP, Kremer P, Hacker S. 1996 Distribution and vertical migration of salps (Tunicata, Thaliacea) near Bermuda. *J. Plankton Res.* **18**, 747–755. (doi:10.1093/plankt/18.5.747)
34. Wiebe PH, Madin LP, Haury LR, Harbison GR, Philbin LM. 1979 Diel vertical migration by *Salpa aspera* and its potential for large-scale particulate organic matter transport to the deep-sea. *Mar. Biol.* **53**, 249–255. (doi:10.1007/BF00952433)
35. Madin LP, Kremer P, Wiebe PH, Purcell JE, Horgan EH, Nemazie DA. 2006 Periodic swarms of the salp *Salpa aspera* in the Slope Water off the NE United States: biovolume, vertical migration, grazing, and vertical flux. *Deep Sea Res. I* **53**, 804–819. (doi:10.1016/j.dsr.2005.12.018)
36. Bianchi D, Galbraith ED, Carozza DA, Mislan KA, Stock CA. 2013 Intensification of open-ocean oxygen depletion by vertically migrating animals. *Nat. Geosci.* **6**, 545–548. (doi:10.1038/ngeo1837)
37. Haddock SH, Heine JN. 2005 Scientific blue-water diving. California Sea Grant College Program.